Large Eddy Simulation Modeling of Turbulent Deflagrations

JUSTIN WILLIAMSON[1], JASON MCGILL[1], and ARNAUD TROUVE[2]
[1] Department of Mechanical Engineering
[2] Department of Fire Protection Engineering
University of Maryland
College Park, MD 20742 (USA)

ABSTRACT

The objective of the present study is to enhance the simulation capability of the Fire Dynamics Simulator (FDS) developed by the National Institute of Standards and Technology, USA, and thereby extend its domain of application towards the treatment of deflagration events in fuel vapor cloud explosions. The proposed deflagration model is based on the filtered reaction progress variable approach, and features a classical flamelet viewpoint combined with an adaptation to a large eddy simulation formulation. The paper discusses the theoretical foundations of the model as well as the numerical difficulties associated with the need to grid-resolve the LES-filtered flame structure. The performance of the LES turbulent deflagration model is also evaluated in a series of benchmark FDS-based simulations corresponding to propagating laminar or turbulent flames.

KEYWORDS: CFD, large eddy simulation, modeling, explosion, deflagration, premixed turbulent combustion

INTRODUCTION

In most situations relevant to fire applications, the combustion occurs in a non-premixed mode in which fuel and air are initially segregated, and the flame location and burning intensity are determined by the fuel-air mixing process. In a number of fire scenarios, however, for instance in situations corresponding to the accidental release and subsequent explosion of vaporized fuel in ambient air [1-4], a significant amount of fuel-air mixing may take place prior to ignition. The mixing process will result in some portions (large or small) of the fuel vapor cloud being within the fuel-air flammability limits. Following ignition, the combustion will proceed in part as a thin deflagration or detonation wave that propagates across the flammable portions of the fuel vapor cloud. We focus in the following on the deflagration scenario, in which the flame propagates at subsonic speeds and pressure remains quasi-uniform across the flame zone.

Our objective in the present study is to develop a Computational Fluid Dynamics solver that can describe turbulent premixed combustion phenomena for fire safety applications (see Refs. [5-7] for a description of similar efforts). The developments are made in the context of an advanced solver called the Fire Dynamics Simulator (FDS). FDS is developed by the National Institute of Standards and Technology, USA, and is oriented towards fire applications; it uses a Large Eddy Simulation (LES) approach for turbulence and an equilibrium-chemistry, mixture-fraction-based model for non-premixed combustion [8,9]. There is currently no premixed combustion modeling capability in FDS.

COPYRIGHT © 2005 INTERNATIONAL ASSOCIATION FOR FIRE SAFETY SCIENCE

In the classical description of premixed combustion, a reaction progress variable c is introduced: c = 0 in the fresh reactants (upstream of the flame), c = 1 in the burnt products (downstream of the flame), and the flame is the region where c goes from 0 to 1 [10-12]. Under the mildly restrictive assumption of equal Lewis numbers, the reactive mixture composition is uniquely mapped in terms of c and the original deflagration modeling problem becomes one of predicting the c-field space and time variations. The reaction progress variable framework is general and flexible, and it has been recently adapted to a LES treatment of propagating turbulent premixed flames [13-21]. The treatment is based on a transport equation for the LES-filtered reaction progress variable $\tilde{c}$, and flame propagation is predicted via the LES-resolved $\tilde{c}$ -field variations.

We consider in the following an extension of the FDS combustion modeling capability to the case of propagating premixed flames using the filtered reaction progress variable approach. While our ultimate objective is to describe deflagrations propagating in fuel-air mixtures with variable composition (as may be found in vapor cloud explosion scenarios), we limit our discussion here to the case of homogeneous fuel-air mixing conditions.

This study is a continuation of the work presented in Ref. [22]. The tests presented in Ref. [22] were preliminary and limited to laminar flames, in the absence of heat release. The new results reported below include laminar and turbulent flames, with full accounting of heat release effects.

DEFLAGRATION MODELING USING THE FILTERED REACTION PROGRESS VARIABLE APPROACH

We start from a simplified description of the combustion transformation via a global, single-step, chemical kinetics equation:

$$\underbrace{C_n H_m O_p}_{F} + (n + \frac{m}{4} - \frac{p}{2}) O_2 \rightarrow n CO_2 + \frac{m}{2} H_2 O \tag{1}$$

where $C_nH_mO_p$ represents the gaseous fuel (also noted F), O_2 the ambient oxygen; and where CO_2 and H_2O are the combustion products. Assuming equal molecular diffusion coefficients (i.e., equal Lewis numbers), it may be shown that the mass fractions of the reactive species are all linearly related and may be expressed in terms of a single reduced mass fraction called the reaction progress variable c [10-12]:

$$c = \frac{(Y_F^u - Y_F)}{(Y_F^u - Y_F^b)} = \frac{(Y_{O_2}^u - Y_{O_2})}{(Y_{O_2}^u - Y_{O_2}^b)} = \frac{Y_{CO_2}}{Y_{CO_2}^b} = \frac{Y_{H_2O}}{Y_{H_2O}^b} \tag{2}$$

or equivalently:

$$\left.\begin{aligned} Y_F &= (1-c) \times Y_F^u + c \times Y_F^b \\ Y_{O_2} &= (1-c) \times Y_{O_2}^u + c \times Y_{O_2}^b \\ Y_{CO_2} &= c \times Y_{CO_2}^b \\ Y_{H_2O} &= c \times Y_{H_2O}^b \end{aligned}\right\} \tag{3}$$

where Y_k is the mass fraction of species k, Y_k^u the value of Y_k in the unburnt gas, and Y_k^b the value of Y_k in the burnt gas. Y_k^u is an input quantity to the combustion problem that characterizes the initial state of the reactive mixture (prior to combustion); Y_k^b is a quantity that characterizes the final mixture composition and that may be obtained from equilibrium thermodynamics. For instance, under fuel lean conditions, we have:

$$Y_F^b = 0 \; ; \; Y_{O_2}^b = Y_{O_2}^u - r_s Y_F^u \; ; \; Y_{CO_2}^b = \eta_{CO_2} Y_F^u \; ; \; Y_{H_2O}^b = \eta_{H_2O} Y_F^u \tag{4}$$

where r_s is the stoichiometric oxygen-to-fuel mass ratio, η_{CO2} the CO_2 species yield (mass of carbon dioxide produced per unit mass of fuel consumed), and η_{H2O} the H_2O species yield (mass of water vapor produced per unit mass of fuel consumed). Similarly, under fuel rich conditions, we have:

$$Y_F^b = Y_F^u - (Y_{O_2}^u / r_s) \; ; \; Y_{O_2}^b = 0 \; ; \; Y_{CO_2}^b = \eta_{CO_2} (Y_{O_2}^u / r_s) \; ; \; Y_{H_2O}^b = \eta_{H_2O} (Y_{O_2}^u / r_s) \tag{5}$$

In the reaction progress variable approach, the reactive mixture composition is calculated as a function of c using Eqs. 3-5, while the c-variations are obtained by solving a classical mass balance equation:

$$\frac{\partial}{\partial t}(\rho c) + \frac{\partial}{\partial x_i}(\rho u_i c) = \frac{\partial}{\partial x_i}(\rho D \frac{\partial c}{\partial x_i}) + \dot{\omega}_c \tag{6}$$

where ρ is the mass density, u_i the x_i-component of the flow velocity vector, D the mass molecular diffusion coefficient (in units of m^2/s), and $\dot{\omega}_c$ the reaction rate (the mass of product formed by combustion, per unit time and per unit volume; in units of $kg/s\text{-}m^3$).

We now consider the implications of Eq. 6 to the treatment of turbulent premixed flames in a LES approach. After applying a LES filter to Eq. 6, we obtain:

$$\frac{\partial}{\partial t}(\overline{\rho}\widetilde{c}) + \frac{\partial}{\partial x_i}(\overline{\rho}\widetilde{u}_i \widetilde{c}) = -\frac{\partial}{\partial x_i}(\overline{\rho u_i c} - \overline{\rho}\widetilde{u}_i \widetilde{c}) + \frac{\partial}{\partial x_i}(\overline{\rho D \frac{\partial c}{\partial x_i}}) + \overline{\dot{\omega}}_c \tag{7}$$

where the over-bar symbol denotes straight LES-filtered quantities; and the tilde symbol denotes Favre-weighted (i.e., mass density weighted) LES-filtered quantities. The first term on the right-hand-side of Eq. 7 represents convective transport of c due to subgrid-scale turbulent fluctuations; the second term represents transport of c due to molecular diffusion; and the last term represents production of c due to chemical reaction.

Using the turbulent eddy viscosity concept and assuming gradient-transport, we may describe the LES-unresolved convective transport of c as [11,12]:

$$(\overline{\rho u_i c} - \overline{\rho}\widetilde{u}_i \widetilde{c}) = -\overline{\rho} \frac{\nu_t}{Sc_t} \frac{\partial \widetilde{c}}{\partial x_i} \tag{8}$$

where ν_t is the Smagorinsky turbulent eddy-diffusivity (in units of m^2/s), and Sc_t a turbulent Schmidt number.

We also adopt a classical flamelet viewpoint and choose to write the volumetric chemical reaction rate as the product of a laminar-like reaction rate per unit flame surface area times a flame surface density [11,12]:

$$\overline{\dot{\omega}_c} = (\rho_u s_L) \times \Sigma \tag{9}$$

where ρ_u is the unburnt gas mass density, s_L the laminar flame speed, and Σ the LES-filtered flame surface-to-volume ratio (in units of 1/m). Following Veynante and co-workers [13-16], we propose to write:

$$\Sigma = \Xi \times 4 \sqrt{\frac{6}{\pi}} \frac{\widetilde{c}(1-\widetilde{c})}{\Delta_c} \tag{10}$$

where Ξ is the subgrid-scale flame wrinkling factor ($\Xi \geq 1$; and $\Xi = 1$ in the absence of subgrid-scale flame surface wrinkling), and where Δ_c is the LES filter size. Equation 10 may also be interpreted as follows:

$$\Sigma = 4 \sqrt{\frac{6}{\pi}} \frac{\widetilde{c}(1-\widetilde{c})}{\Delta_c} + (\Xi - 1) \times 4 \sqrt{\frac{6}{\pi}} \frac{\widetilde{c}(1-\widetilde{c})}{\Delta_c} \tag{11}$$

where the first term on the right-hand-side represents the LES-resolved component of flame surface density, and the second term the subgrid-scale component. The relative weight between those two components depends on the value of Ξ with respect to 1. While elaborate closure model expressions have been recently proposed in the scientific literature to describe the flame wrinkling factor [23-24], we choose in the present study to neglect the subgrid-scale component entirely and assume $\Xi = 1$. This simplification is proposed as a temporary expedient and clearly needs to be removed in future work.

Equation 7 also requires a physical submodel for the molecular transport of c. While the contribution of molecular diffusion is expected to be small in flame regions where the turbulence intensity is high, this contribution will be significant, and possibly dominant, in regions where the turbulence intensity is low. In Ref. [16], the Kolmogorov-Petrovskii-Piskunov (KPP) theory [25-28] is used to establish a suitable closure model for molecular diffusion: it is shown that this closure model is constrained by the modeling choices made in the description of the chemical source term in Eqs. 9-10; the constraint comes from the realizability requirement that under laminar flow conditions (i.e., under conditions in which $\nu_t = 0$ and $\Xi = 1$), the flame propagates at the laminar flame speed s_L. We adopt in the following the closure model of Refs. [15,16] and write:

$$\overline{\rho D \frac{\partial c}{\partial x_i}} = \frac{\rho_u s_L \Delta_c}{16\sqrt{6/\pi}} \frac{\partial \widetilde{c}}{\partial x_i} \tag{12}$$

The final expression of the transport equation for the (Favre-weighted) LES-filtered reaction progress variable is then:

$$\frac{\partial}{\partial t}(\overline{\rho}\widetilde{c}) + \frac{\partial}{\partial x_i}(\overline{\rho}\widetilde{u}_i\widetilde{c}) = \frac{\partial}{\partial x_i}\left(\left(\overline{\rho}\frac{\nu_t}{Sc_t} + \frac{\rho_u s_L \Delta_c}{16\sqrt{6/\pi}}\right)\frac{\partial \widetilde{c}}{\partial x_i}\right) + (\rho_u s_L)\Xi \times 4\sqrt{\frac{6}{\pi}}\frac{\widetilde{c}(1-\widetilde{c})}{\Delta_c} \tag{13}$$

This partial differential equation features a classical convection-diffusion-reaction structure and may be easily handled by Computational Fluid Dynamics solvers. It is also possible to gain further insight into the model formulation in Eq. 13 by using the

analytical methods of the KPP theory [25-28]. We find that Eq. 13 implies the following expression for the local propagation velocity of the LES-filtered flame:

$$s_t = s_L \sqrt{\Xi \times (1 + \frac{\nu_t}{Sc_t} \frac{16\sqrt{6/\pi}}{s_L \Delta_c})} \qquad (14)$$

This expression conveniently illustrates some of the main features of the proposed filtered-*c* approach. First, as mentioned above, in the absence of subgrid-scale turbulence ($\nu_t = 0$ and $\Xi = 1$), the flame propagates at the laminar speed s_L. Second, in the presence of subgrid-scale turbulence ($\nu_t > 0$ and $\Xi > 1$), s_t is increased by a variable factor and this factor depends on local turbulence properties, as measured by the flame wrinkling factor and the turbulent eddy-diffusivity. In the present study, we use the simplification $\Xi = 1$, and the local flame propagation velocity is a unique function of the pseudo-Reynolds number $(s_L \Delta_c / \nu_t)$.

Next, we discuss the grid resolution requirement of the model formulation in Eq. 13, and the relationship between the LES filter size Δ_c and the computational grid cell size Δ (in FDS, Δ is defined as the cubic root of the grid cell volume). As discussed in Refs. [13-18], the local thickness of the LES-filtered flame (i.e., the local gradient-thickness of the spatial $\tilde{c}$ -variations) is of order Δ_c and the flame is numerically correctly resolved on the computational grid for length scale ratios (Δ_c/Δ) much larger than one. A ratio equal to or smaller than one will result in stiff spatial variations of $\tilde{c}$ and subsequent numerical difficulties. In Refs. [13-18], the recommended values are such that $(\Delta_c/\Delta) \geq 5$.

Note that the grid resolution requirement of the filtered-*c* approach is higher than that associated with the turbulence model. For instance, let us call Δ_u the LES filter size used in the momentum equations; the standard Smagorinsky model uses $(\Delta_u/\Delta) = 1$. The differences between the required values of (Δ_c/Δ) and (Δ_u/Δ) illustrate that in LES, it is harder to resolve the flame than to resolve the flow. A consistent LES treatment calls for using a single filter size, $\Delta_u = \Delta_c$. This choice, however, corresponds to a prohibitive increase in computational cost: for instance, while a flow calculation without combustion may be performed with a relatively coarse grid, $\Delta = \Delta_u$, the same calculation with combustion will require a much denser grid, $\Delta \leq (\Delta_u/5)$, i.e., a grid refinement by a factor of at least $5^3 = 125$. This is generally viewed as an excessive burden and current implementations of the filtered-*c* model adopt a more cost-effective approach in which 2 different filter sizes are used, for example: $\Delta_c = (5 \times \Delta_u)$ and $(\Delta_u/\Delta) = 1$. While the choice of 2 different filters introduces inconsistencies and errors, we choose here to ignore these errors and consider in the following the ratio (Δ_c/Δ_u) as a free model parameter. The exact implications of this simplification will be addressed in future work.

The filtered-*c* model and the corresponding partial differential Eq. 13 have been implemented into FDS and we now present some validation test results that correspond to homogeneous, laminar or turbulent deflagrations.

FDS SIMULATIONS OF LAMINAR DEFLAGRATIONS

We consider in this section a simple test configuration corresponding to a one-dimensional, plane, laminar, premixed flame that propagates along the *x*-direction into an homogeneous fuel-air mixture (Fig. 1). The computational domain is $(50 \times 1 \times 1)$ m^3 and

the numerical boundaries are fully open. The computational grid corresponds to a uniform rectangular mesh; its size is $(500 \times 10 \times 10)$, which corresponds to cubic cells with a 10 cm x-length. At initial time, the fuel-air mixture is assumed to be at rest and in a chemically frozen state ($\widetilde{c}$ = 0). Flame initiation is triggered by a numerical ignitor located near x = 50 m; this numerical ignitor is modeled as a spatially- and temporally-localized extra source term introduced into Eq. 13. The laminar flame speed is set to s_L = 0.5 m/s.

The deflagration model is coupled to the FDS statements for mass, momentum and energy conservation [8,9] via a modified description of the heat release rate:

$$\overline{\dot{q}} = \overline{\dot{\omega}}_c \times (Y_F^u - Y_F^b)\Delta H_F \tag{15}$$

where ΔH_F is the heat of combustion (energy released per unit mass of fuel consumed; in units of J/kg). The heat of combustion is here specified so that the adiabatic flame temperature is 2250 K. Finally, while the configuration is treated as fully three-dimensional, the results do confirm that the flame and flow structure have negligible y- and z-variations.

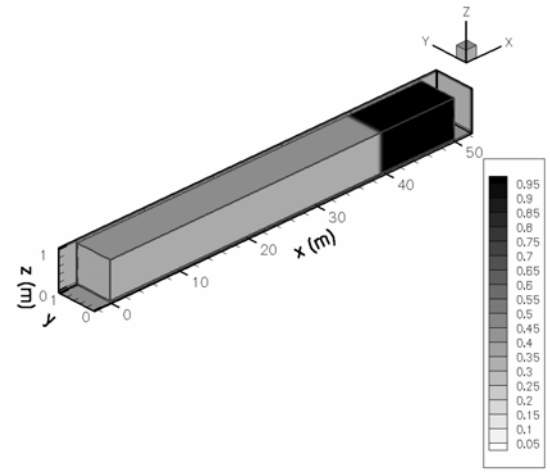

Fig. 1. Numerical configuration corresponding to a one-dimensional, plane, laminar deflagration. The flame is numerically ignited near x = 50 m and propagates in the negative x-direction. The plot shows the instantaneous spatial distribution of the filtered reaction progress variable, 10 seconds after ignition.

Figure 2 presents a series of numerical results performed for different values of the filter-to-grid length scale ratio, $2 \leq (\Delta_c/\Delta) \leq 8$. Figure 2a gives the time history of flame speed, while Figs. 2b-d present instantaneous profiles that reveal the main features of the flame structure.

The flame speed plotted in Fig. 2a is obtained by monitoring the time variations of the total burnt gas volume V_b:

$$V_b(t) = \iiint_V \widetilde{c}(x, y, z, t)dxdydz \tag{16}$$

where spatial integration is performed over the whole computational volume V. The numerical flame speed s_L^* may then be calculated as:

$$s_L^* = \frac{1}{S}\frac{dV_b}{dt} \tag{17}$$

where S is the configuration y-z cross-section area, $S = 1$ m^2.

All curves in Fig. 2a exhibit a transient phase during which the simulated flame structure evolves from initial to final shape; the exact duration τ of this transient phase depends on the details of the ignition process as well as on the grid cell size, and is found in our particular case to be relatively long, $\tau \approx$ 10-20 s. After this initial transient phase, the LES flame structure achieves steady-state and the value of s_L^* remains approximately constant (this value is compared in Fig. 2a to the user-specified exact value $s_L = 0.5$ m/s). The steady-state value of s_L^* is found to depend on how well the LES-filtered flame is resolved by the computational grid. For large values of the filter-to-grid length scale ratio, $(\Delta_c/\Delta) \geq 4$, the flame speed is somewhat over-estimated but the error remains less than 20%; note that higher levels of accuracy are gradually achieved when increasing the ratio (Δ_c/Δ). In contrast, for small values of the filter-to-grid length scale ratio, $(\Delta_c/\Delta) = 2$, the flame speed is not correctly predicted and does not appear to have a well-defined stable value.

The importance of the filter-to-grid length scale ratio is further illustrated in Figs. 2b and 2c. Figure 2b presents the spatial variations of the LES-filtered reaction progress variable across the flame. These profiles are taken at arbitrarily chosen times in the simulations, after steady-state flame propagation has been achieved. The profiles are plotted for three different levels of flame resolution, ranging from high to low. For $(\Delta_c/\Delta) = 8$, the sharp $\widetilde{c}$ -gradient that develops at the flame location is resolved by more than 10 grid cells and therefore remains smooth on the computational grid. In contrast, for $(\Delta_c/\Delta) = 2$, the $\widetilde{c}$ -gradient is resolved by only 3 grid cells and is numerically stiff; this numerical stiffness explains the tendency to develop numerical oscillations and the severe loss of accuracy observed in Fig. 2a.

Figure 2c is similar to Fig. 2b and focuses on temperature variations across the flame. A comparison between Figs. 2b and 2c emphasize the strong relationship between reaction progress variable and temperature that holds for adiabatic systems [10-12]. Note that irrespective of resolution issues, all simulated flames release the correct amount of heat and the temperature downstream of the flame is the user-specified adiabatic flame temperature $T_b \approx 2250$ K.

Figure 2d presents the spatial variations of the LES-filtered x-component of flow velocity across the flame and is used to evaluate the ability of the deflagration model to predict the correct amount of thermal dilatation. As seen in Fig. 2d, while the fuel-air mixture remains at rest upstream of the flame (for small values of x), flame-induced thermal dilatation triggers flow motion and establishes a flow of combustion products in the downstream region (at large values of x). It may be shown that for a flame propagating into a quiescent mixture, the burnt gas flow velocity u_b is a function of both the density ratio between unburnt and burnt gas, and the laminar flame speed [10,11]:

$$u_b = (\frac{\rho_u}{\rho_b} - 1) \times s_L \tag{18}$$

We find $u_b \approx 3.34$ m/s. This value is plotted in Fig. 2d and is conveniently used to graphically evaluate the quality of each predicted flame structure. Well-resolved flames, i.e., $(\Delta_c/\Delta) \geq 4$, are found to produce downstream flow velocities that are close to the theoretical value, whereas under-resolved flames, i.e., $(\Delta_c/\Delta) = 2$, lead to large errors and incorrect (non-monotonic) flow structures.

In summary, these test results agree well with previous work from the literature [13-18] and emphasize the importance of flame resolution, as measured by the filter-to-grid length scale ratio. The recommended value is such that $(\Delta_c/\Delta) \geq 5$.

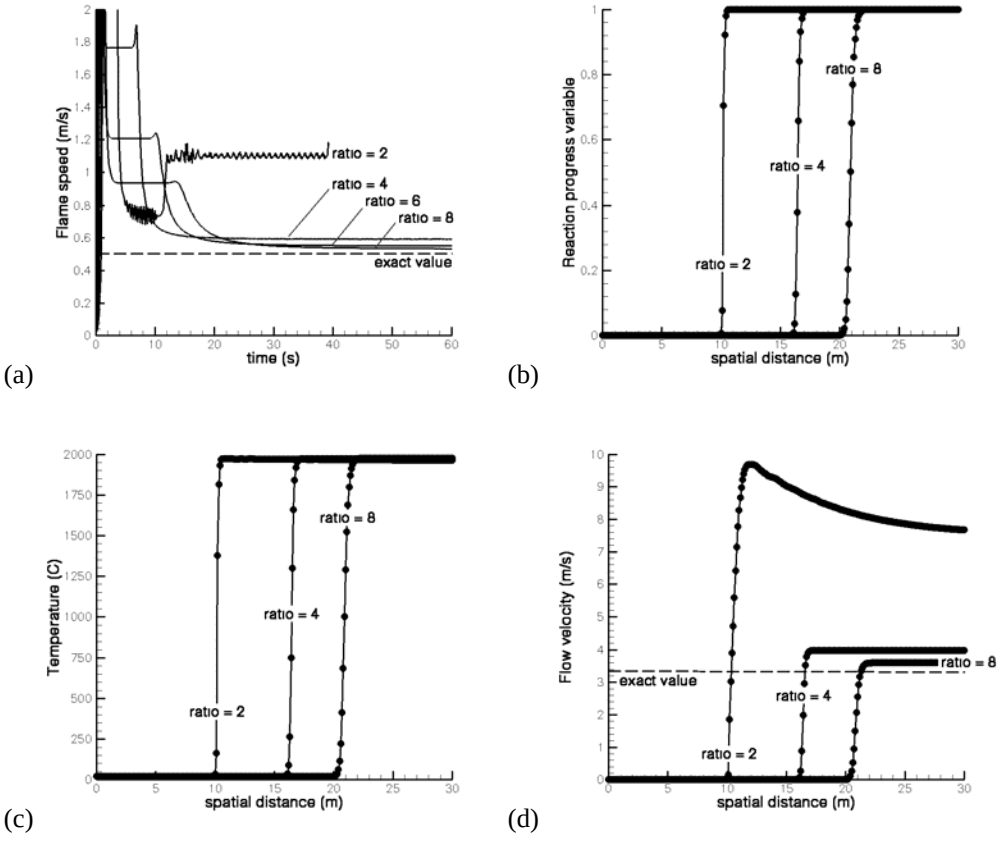

Fig. 2. Flame speed and flame structure in FDS simulations of one-dimensional, plane, laminar deflagrations. The different solutions correspond to different values of the filter-to-grid length scale ratio. (a) Flame speed versus time; (b) Spatial variations of reaction progress variable; (c) Spatial variations of temperature; (d) Spatial variations of flow velocity.

FDS SIMULATIONS OF TURBULENT DEFLAGRATIONS

We consider in this section another basic test configuration corresponding to a turbulent premixed flame stabilized downstream of a bluff-body in a wind tunnel set-up (Fig. 3).

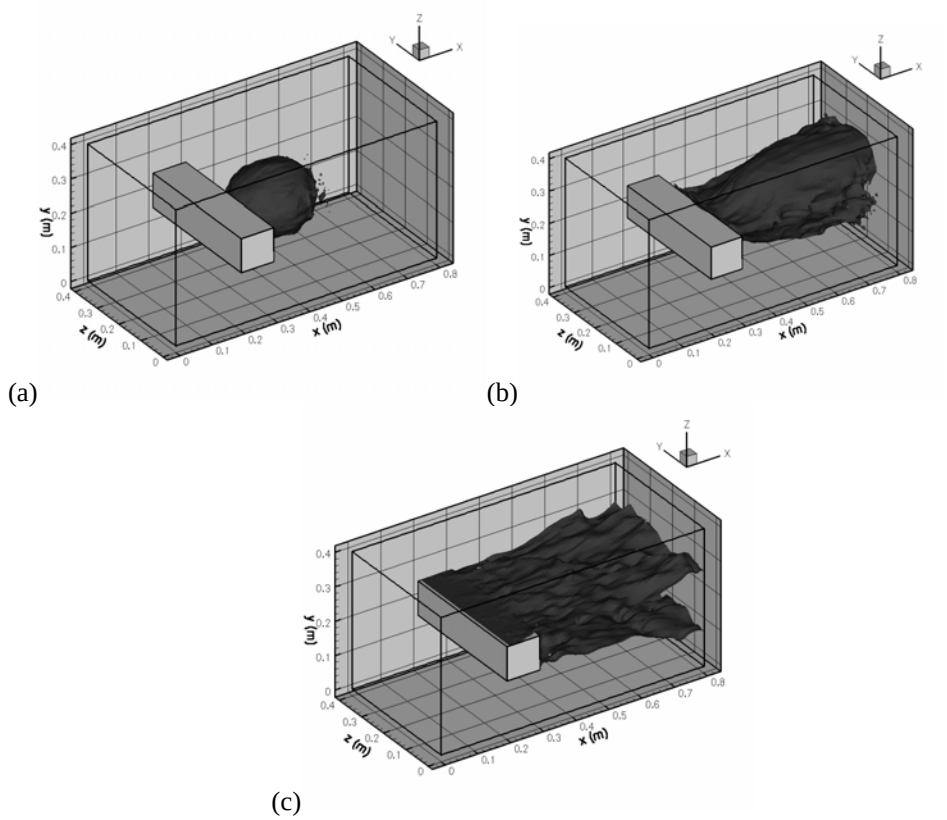

(a) (b)

(c)

Fig. 3. Successive instantaneous snapshots of the flame surface from the FDS simulation of flame ignition in a wind tunnel set-up featuring a square-shaped cylinder. The flow direction is from left to right. The flame is defined as the isocontour $\widetilde{c}$ = 0.9. (a) Flame ignition; (b) Transition to a fully-developed turbulent flame; (c) Successful flame stabilization.

The incoming flow corresponds to an homogeneous fuel-air mixture moving at a uniform velocity equal to U = 5 m/s; the bluff body is a square-shaped cylinder and its dimension is H =0.1 m; the flow Reynolds number if $Re_H = (U \times H/\nu) \approx 31{,}000$. The computational domain is $(0.8 \times 0.4 \times 0.4)$ m^3 and the numerical boundaries are fully open. The computational grid corresponds to a uniform rectangular mesh; its size is $(80 \times 40 \times 40)$, which corresponds to cubic grid cells with a 1 cm^3 volume. At initial time, the fuel-air mixture is assumed to be in a chemically frozen state ($\widetilde{c}$ = 0); and flame initiation is triggered by a numerical ignitor located in the wake of the bluff body. Note that prior to ignition, the FDS solution is allowed to develop a classical turbulent wake flow structure characterized by quasi-periodic shedding of large vortices of size comparable to H. The size of these large vortices correspond to approximately 10 grid cells, which is arguably

on the lean-side of a typical LES requirement [11,12], but is considered acceptable for the present purpose. The laminar flame speed is s_L = 0.5 m/s; the heat of combustion is such that the adiabatic flame temperature is 2250 K. The filter-to-grid length scale ratio is $(\Delta_c/\Delta) = 6$.

Figure 3 presents a sequence of three successive snapshots of the flame surface that are representative of the double transition observed in the simulation. In Fig. 3, the flame is identified as a $\tilde{c}$ -field iso-level; we use $\tilde{c}$ = 0.9. Figure 3a shows the early laminar-like spherical flame kernel that develops close to the ignition source, in the wake of the square-shaped cylinder. The next image in Fig. 3b shows a rapid transition to a fully-developed turbulent (i.e., wrinkled) flame. At this point, most of the flame dynamics still takes place away from the cylinder walls, and it remains unclear whether the flame will achieve successful stabilization or be simply blown off. This question is answered in Fig. 3c: Fig. 3c shows that the flame successfully achieves stabilization and attaches to the square-shaped cylinder (note that the flame is observed to propagate inside the flow boundary layers on the cylinder upper and lower wall surfaces).

These test results are found to be very encouraging and the simulated flame dynamics shown in Fig. 3 are consistent with the known dynamics of turbulent deflagrations, as observed in laboratory-scale experiments [10-12]. Future work will be aimed at performing more quantitative tests of the new FDS deflagration modeling capability.

CONCLUSION

An advanced deflagration model based on the filtered reaction progress variable approach has been implemented into FDS. The domain of validity of the model corresponds to the laminar flamelet regime of turbulent premixed combustion, a regime that is expected to apply to most situations of engineering interest in fire safety applications. The model has been tested in several basic configurations corresponding to propagating, homogeneous, laminar or turbulent premixed flames. Particular attention has been paid to the grid resolution requirement of the proposed model formulation, and to the relationship between the LES filter size Δ_c and the computational grid cell size Δ. The local thickness of the simulated flame is of order Δ_c and the flame is numerically correctly resolved on the computational grid for length scale ratios (Δ_c/Δ) much larger than one. A ratio equal to or smaller than one will result in stiff spatial variations of the reaction progress variable and subsequent numerical difficulties (i.e., large numerical errors). The numerical tests performed in the present study suggest that the proposed FDS deflagration model requires a filter-to-grid length scale ratio equal to or greater than 4, $(\Delta_c/\Delta) \geq 4$.

The results are found to be encouraging and current work is aimed at extending the FDS deflagration modeling capability to cases with non-homogeneous fuel-air mixture composition and partially-premixed combustion.

ACKNOWLEDGMENTS

This work is supported by the U.S. Naval Surface Warfare Center, Indian Head Division.

REFERENCES

[1] Strehlow, R.A., “Unconfined Vapor-Cloud Explosions – An Overview,” *Proceedings of the Combustion Institute*, **14**: pp. 1189-1200, (1973).

[2] Baker, W.E., and Tang, M.J., *Gas, Dust and Hybrid Explosions*, Elsevier, 1991.

[3] Bradley, D., Cresswell, T.M., and Puttock, J.S., "Flame Acceleration Due to Flame-Induced Instabilities in Large-Scale Explosions," *Combustion and Flame*, **124**: pp. 551-559, (2001).

[4] Zalosh, R., "Explosion Protection," *The SFPE Handbook of Fire Protection Engineering*, National Fire Protection Association (3rd ed.), 2002, pp. 3/402-3/421.

[5] Molkov, V., Makarov, D., Ryzhov, A., and Duval, A., "Modelling and Simulations of Large-scale Accidental Combustion," *Proceedings of the Technical Congress on "Computational Simulation Models in Fire Engineering and Research,"* University of Cantabria, Santander, Spain, 2004, pp. 315-341.

[6] Molkov, V., Makarov, D., and Grigorash, A., "Cellular Structure of Explosion Flames: Modelling and Large-Eddy Simulation," *Combustion Science and Technology*, **176**: pp. 851-865, (2004).

[7] Cant, R.S., Dawes, W.N., and Savill, A.M., "Advanced CFD and Modeling of Accidental Explosions," *Annual Review of Fluid Mechanics*, **36**: pp. 97-119, (2004).

[8] McGrattan, K.B., "Fire Dynamics Simulator (Version 4). Technical Reference Guide," National Institute of Standards and Technology NIST Special Publication 1018, Gaithersburg, MD, 2004.

[9] McGrattan, K., Floyd, J., Forney, G., Baum, H., and Hostikka, S., "Improved Radiation and Combustion Routines for a Large Eddy Simulation Fire Model," *Fire Safety Science – Proceedings of the Seventh International Symposium*, International Association for Fire Safety Science, 2003, pp. 827-838.

[10] Williams, F.A., *Combustion Theory*, Benjamin/Cummings (2nd ed.), 1985.

[11] Poinsot, T., and Veynante, D., *Theoretical and Numerical Combustion*, Edwards (2nd ed.), 2004.

[12] Veynante, D., and Vervisch, L., "Turbulent Combustion Modeling," *Progress in Energy and Combustion Science*, **28**: pp. 193-266, (2002).

[13] Boger, M., Veynante, D., Boughanem, H., and Trouvé, A., "Direct Numerical Simulation Analysis of Flame Surface Density Concept for Large Eddy Simulation of Turbulent Premixed Combustion," *Proceedings of the Combustion Institute*, **27**: pp. 917-925, (1998).

[14] Charlette, F., Trouvé, A., Boger, M., and Veynante, D., "A Flame Surface Density Model for Large Eddy Simulations of Turbulent Premixed Flames," *Joint Meeting of the British, German and French Sections of the Combustion Institute*, Combustion Institute, Nancy, France, 1999.

[15] Boger, M., and Veynante, D., "Large Eddy Simulation of a Turbulent Premixed V-Shaped Flame," *Advances in Turbulence*, Dopazo C. (ed.), Cimne, Barcelona, 2000, pp. 449-452.

[16] Boger, M., "Modélisation de Sous-Maille pour la Simulation aux Grandes Echelles de la Combustion Turbulente Prémélangée," *Ph.D. Thesis*, Ecole Centrale Paris, France, 2000.

[17] Hawkes, E.R., and Cant, R.S., "A Flame Surface Density Approach to Large-Eddy Simulation of Premixed Turbulent Combustion," *Proceedings of the Combustion Institute*, **28**: pp. 51-58, (2000).

[18] Hawkes, E.R., and Cant, R.S., "Implications of a Flame Surface Density Approach to Large Eddy Simulation of a Premixed Turbulent Combustion," *Combustion and Flame*, **126**: pp. 1617-1629, (2001).

[19] Tullis, S., and Cant, R.S., "Scalar Transport Modeling in Large Eddy Simulation of Turbulent Premixed Flames," *Proceedings of the Combustion Institute*, **29**: pp. 2097-2104, (2002).

[20] Knikker, R., Veynante, D., and Meneveau, C., "A Priori Testing of a Similarity Model for Large Eddy Simulations of Turbulent Premixed Combustion," *Proceedings of the Combustion Institute*, **29**: pp. 2105-2111, (2002).

[21] Kirkpatrick, M.P., Armfield, S.W., Masri, A.R., and Ibrahim, S.S. "Large Eddy Simulation of a Propagating Turbulent Premixed Flame," *Flow, Turbulence and Combustion*, **70**: pp. 1-19, (2003).

[22] Williamson, J., McGill, J., and Trouvé, A., "A Filtered Progress Variable Approach to Model Turbulent Premixed Combustion in FDS," *Proceedings of the Technical Congress on "Computational Simulation Models in Fire Engineering and Research,"* University of Cantabria, Santander, Spain, 2004, pp. 7-16.

[23] Charlette, F., Meneveau, C., and Veynante, D., "A Power-Law Flame Wrinkling Model for LES of Premixed Turbulent Combustion. Part I: Non-Dynamic Formulation and Initial Tests," *Combustion and Flame*, **131**: pp. 159-180 (2002).

[24] Charlette, F., Meneveau, C., and Veynante, D., "A Power-Law Flame Wrinkling Model for LES of Premixed Turbulent Combustion. Part II: Dynamic Formulation," *Combusion and Flame*, **131**: pp. 181-197, (2002).

[25] Kolmogorov, A.N., Petrovskii, I.G., and Piskunov, N.S., *Bjul. Moskovskovo Gos Univ.*, **1**: pp. 1-72, (1937).

[26] Hakberg, B., and Gosman, A.D., "Analytical Determination of Turbulent Flame Speed From Combustion Models," *Proceedings of the Combustion Institute*, **20**: pp. 225-232, (1984).

[27] Duclos, J.M., Veynante, D., and Poinsot, T., "A Comparison of Flamelet Models for Premixed Turbulent Combustion," *Combustion and Flame*, **95**: pp. 101-117, (1993).

[28] Fichot, F., Lacas, F., Veynante, D., and Candel, S.M., "One-Dimensional Propagation of a Premixed Turbulent Flame with a Balance Equation for the Flame Surface Density," *Combustion Science and Technology*, **90**: pp. 35-60, (1993).